PLANCK 2011, LISBON
1 June 2011

Mini black-holes at RHIC and LHC

Elias Kiritsis

University of Crete APC, Paris

Collaborators

My Collaborators

- A. Taliotis (Crete)
- P. Romatchke (Frankfurt)

Based also on earlier works by

U. Gursoy, L. Mazzanti, F. Nitti

arXiv:1006.5461 [hep-th]

arXiv:0903.2859 [hep-th]

arXiv:0812.0792 [hep-th]

Introduction

• Gravity has been in the focus of high-energy physicists for the past 25 years.

• String theory has played a central role in this.

• Cosmological observations in the last 15 years made a very clear point: we understand very little about gravitational physics and how it ties together with QFT.

• A fascinating ingredient of general relativity and its avatars have been black holes, with their mysterious laws of thermodynamics and the ensuing information paradox (that remains unsettled todate).

• The possibility that black holes exist in the universe, and can be observed, has become real with many related data coming from galactic and extra-galactic astrophysics.

• Such data are necessarily very indirect and rely on matter falling into BHs.

• It was therefore a radical view when it was proposed that mini-black-holes could be produced in colliders like LHC.

Antoniadis+Arkani-Hamed+Dimopoulos+Dvali, Dvali+Kolanovic+Nitti, Giddings+Thomas, Dimopoulos+Landsberg

• The crucial ingredient that made such a possibility, thinkable, was the realization that in gravitational theories with branes, like string theory, the fundamental gravity scale could be as low as a TeV, if the compactification scale is finely (and unnaturally) tuned.

Arkani-Hamed+Dimopoulos+Dvali, Antoniadis+Arkani-Hamed+Dimopoulos+Dvali

• This was possible if space has additional dimensions that are sufficiently large to make M_P small, and sufficiently small to have been hidden todate.

• Another possibility also appeared:Extra dimensions that are warped, and which could still generate a small higher dimensional M_P.

Randall+Sundrum

• The possibility of mini-bhs looked exotic then, and so does today, even more so, as the constraints on the "quantum gravity" scale have become tighter.

Preview

• I will argue today that mini-black holes in one extra dimension have been produced and studied for about 10 years at the RHIC collider.

• Such black holes continue to be produced copiously and studied during the heavy ion collisions at LHC.

• The mini-black holes are not the ones expected from standard higher dimensional gravity. They come from a five-dimensional gravitational theory that is visible only by the strong interactions (QCD).

• Nastase has made such a claim 3 years ago, but his model (based on earlier work by Giddings) using a crude holographic model, and had a part of the story.

• Today, the data are known better and have been analyzed in more detail, and our understanding of the holographic physics of QCD is much more refined.

• The properties of mini-black holes share similarities and differences with the analysis of their features by Giddings and Thomas.

The similarities:

♠ They have a very large total cross section.

♠ Very large multiplicity events, but with few hard final particles

♠ Suppression of hard perturbative scattering processes.

♠ Democratic primary decay (in the strong interactions).

The differences:

♠ Instead of high sphericity events, there is approximately Bjorken boost invariance.

♠ They are BHs in asymptotically AdS space (almost) instead of in asymptotically flat space.

♠ Their primary decay is not via Hawking radiation but via bubble nucleation.

♠ The ratio of hadrons to leptons is small.

The reason for the differences is: the BHs are in a curved space, and the theory contains also other fields (in particular a dilatonic scalar).

RHIC collision

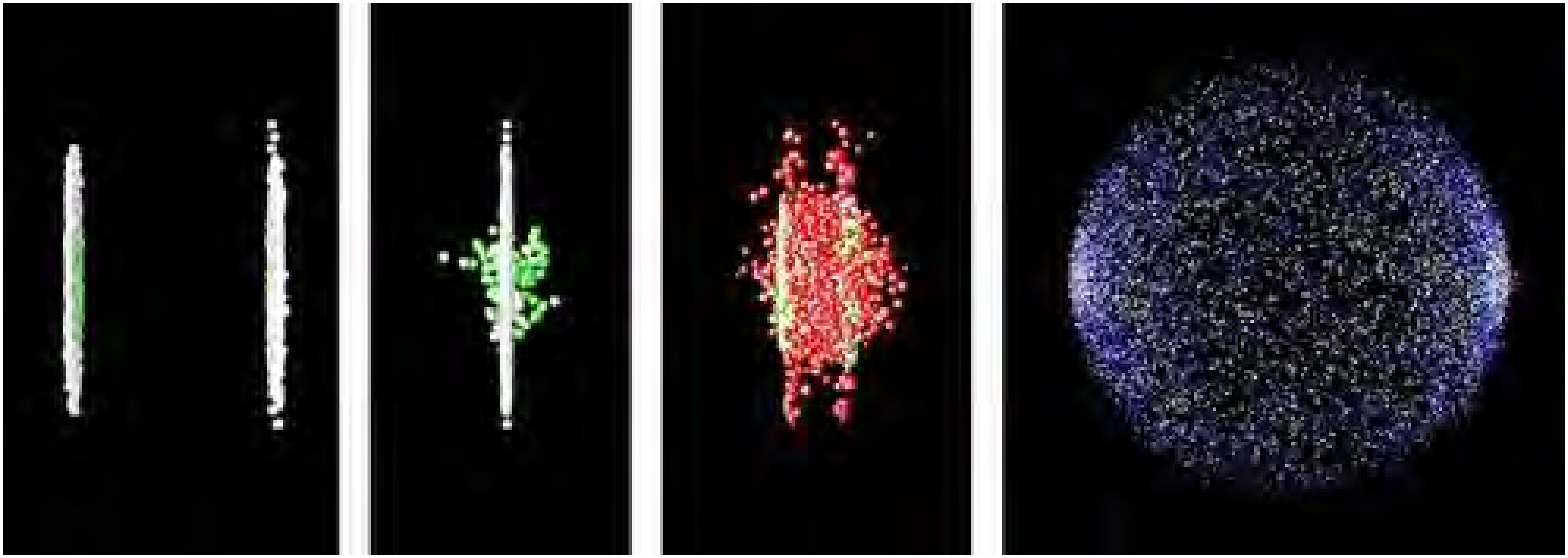

Phases of a collision

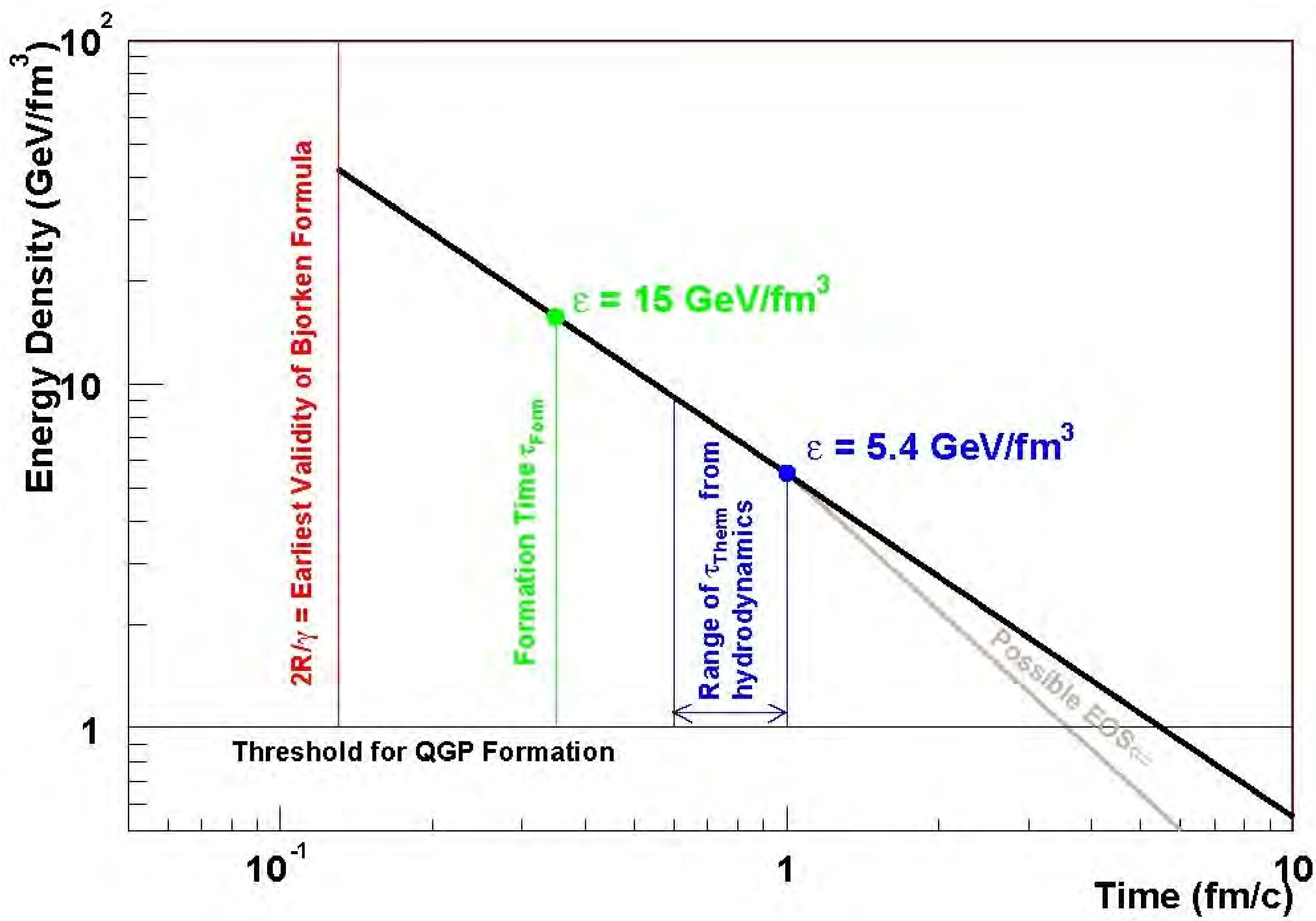

The "initial" energy density is given by the Bjorken formula

Is there thermal equilibrium?

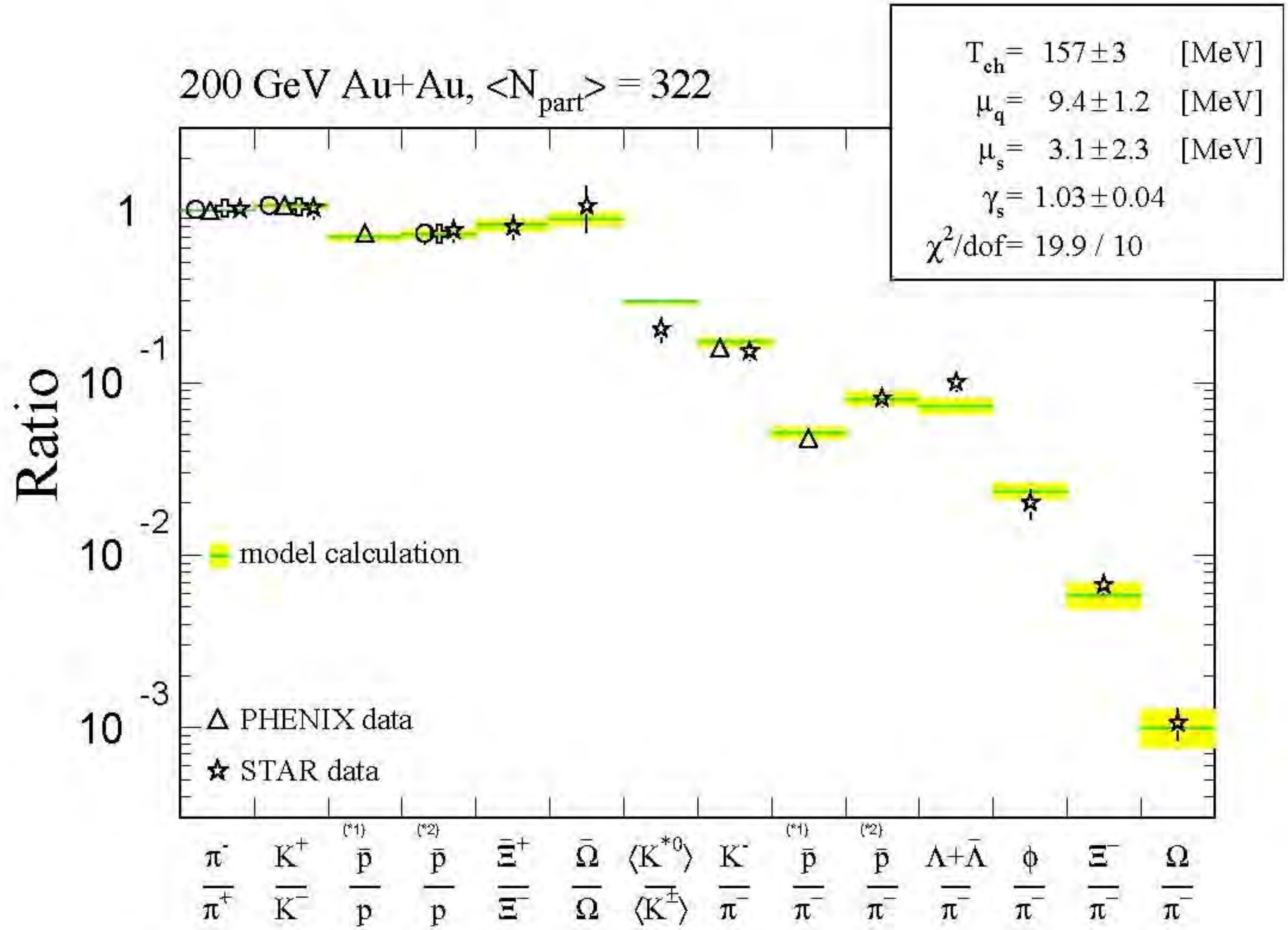

PHENIX (triangles), STAR(stars), BRAHMS (circles) PHOBOS (crosses) particle ratios, at Au+Au (s=200 GeV) at mid-rapidity vs thermal ensemble predictions.

Hydrodynamic elliptic flow

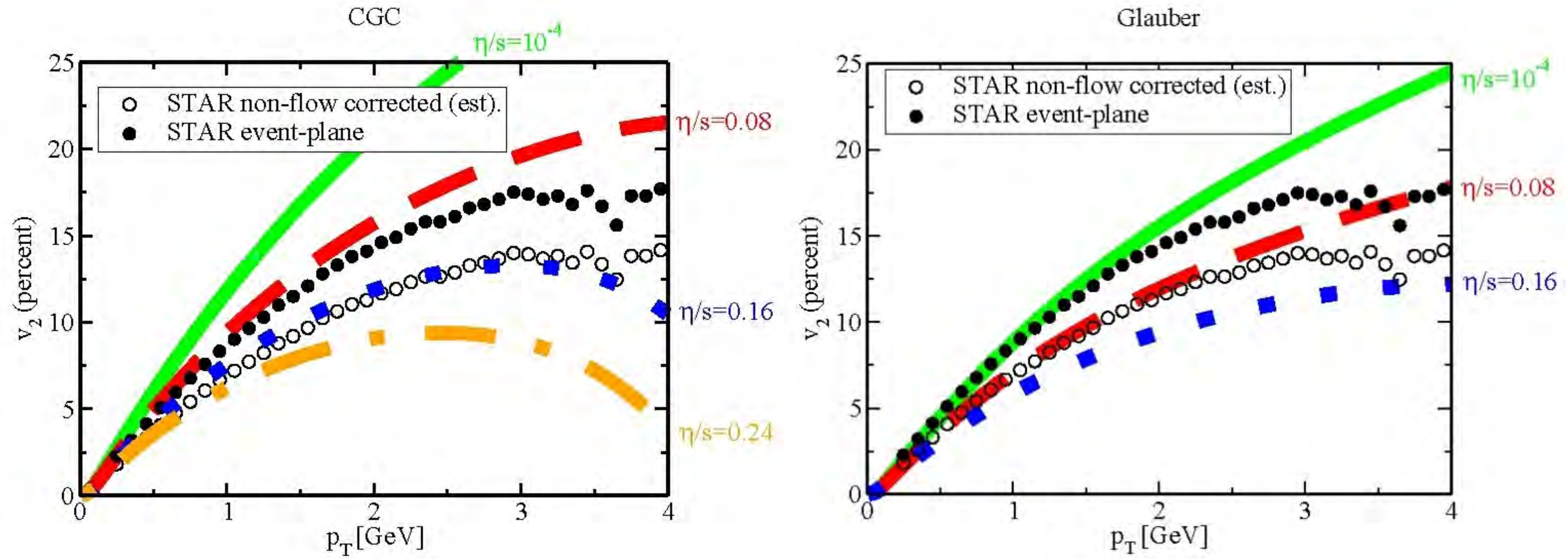

Elliptic flow data from STAR as a function of p_T (right) compared to relativistic hydrodynamics calculations with non-zero shear viscosity, from Luzum+Romanschke (2008).

- Finite-temperature (equilibrium) relativistic hydrodynamics describes well the data with

$$\frac{\eta}{s} \simeq (0.08 - 0.16)\ \hbar \simeq (1-2)\frac{\hbar}{4\pi}$$

Improved Holographic QCD

• A holographic model for YM, that should be reliable at least in the IR, must contain at least a metric (dual to $T_{\mu\nu}$) and a scalar ϕ (the dilaton, dual to $tr[F^2]$). Other operators can be approximately neglected.

• $e^{\phi} \sim \lambda$ at least in the UV.

• A general 2-derivative action is (after field redefinitions)

$$S_{\text{Einstein}} = M^3 N_c^2 \int d^5x \sqrt{g} \left[R - \frac{4}{3} \frac{(\partial\lambda)^2}{\lambda^2} + V(\lambda) \right] \quad , \quad \lambda = N_c \, e^{\phi}$$

The IR asymptotics

• The solutions in the IR either asymptote to AdS_5 (extremum of V) or have a naked singularity.

• In holography naked singularities are acceptable if they satisfy the Gubser bound (they are resolvable).

• They are also computationally reliable if they are "repulsive".

• We also demand confinement, a mass gap and a discrete spectrum.

♠ Parametrize

$$V(\lambda) \sim \lambda^{Q} \, (\log \lambda)^{P} \qquad as \qquad \lambda \to \infty$$

• There is confinement, discrete spectrum and a mass gap for $Q \geq \frac{4}{3}$

• The IR singularity passes the Gubser bound if $Q < \frac{8}{3}$

• There are linear Regge trajectories when $Q = 4/3$ and $P = 1/2$. This is the case the is closer to YM

General phase structure at finite temperature

• For a general monotonic potential (with no minimum) the following are true :

i. *There exists a phase transition at finite $T = T_c$, if and only if the zero-T theory confines.*

Gursoy+Kiritsis+Mazzanti+Nitti (2009)

ii. *This transition is first order for all of the confining geometries, with a single exception (linear dilaton in the IR, continuous spectrum with a gap). The transition is continuous or BKT depending on subleading terms in the potential*

Gursoy+Kiritsis+Mazzanti+Nitti (2009), Gursoy (2010)

iv. *All of the non-confining geometries at zero T are always in the black hole phase at finite T. They exhibit a second order phase transition at $T = 0^+$.*

Temperature versus horizon position

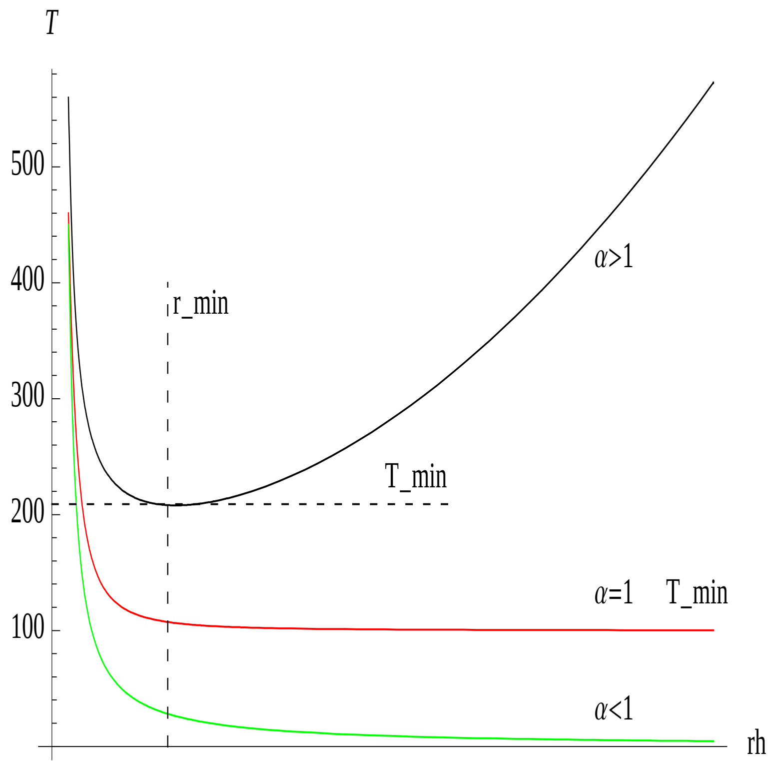

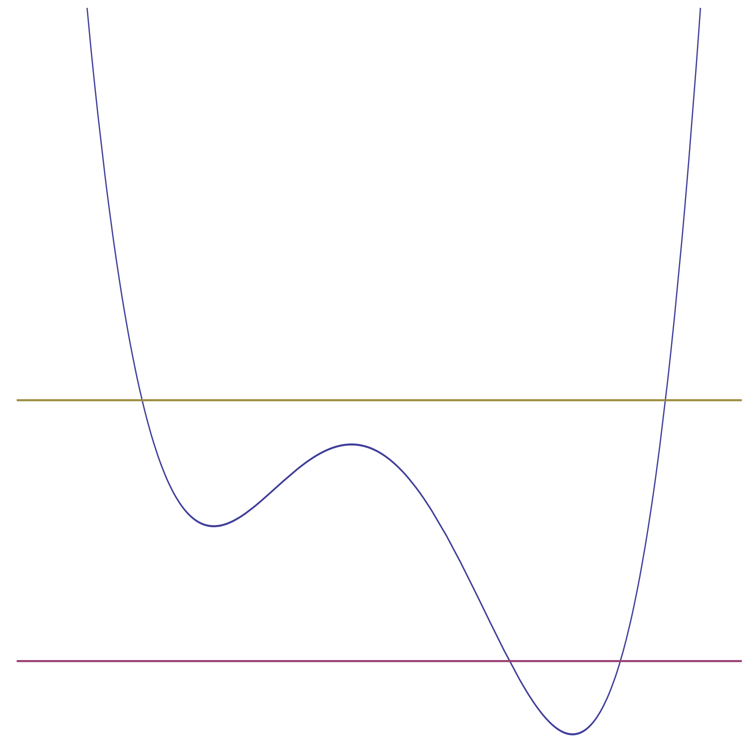

• We plot the relation $T(r_h)$ for various potentials parameterized by a. $a = 1$ is the critical value below which there is only one branch of black-hole solutions.

• For more complicated potentials multiple phase transitions are possible.

Gursoy+Kiritsis+Mazzanti+Nitti (2009), Alanen+Kajantie+Tuominen (2010)

The thermodynamics of small vs large BHs

For $V \sim^{\frac{4}{3}\phi} \phi^{\frac{a-1}{a}}$, $a > 1$ we obtain ($a = 2$ has linear Regge trajectories and describes best YM)

• Large BH branch: asymptotic AdS BHs as $T \to \infty$ with , $r_h \sim T$ $E \sim T^4$ and $S \sim T^3$

• Small BH branch: asymptotic AdS BHs as $T \to \infty$, with $r_h \sim \left(\frac{T}{\Lambda_{YM}}\right)^{\frac{1}{a-1}}$

$$S \simeq V_3 e^{-3\left(\frac{T}{\Lambda_{YM}}\right)^{\frac{a}{a-1}}} \quad , \quad E \simeq M_P^3 V_3 \; T \; e^{-3\left(\frac{T}{\Lambda_{YM}}\right)^{\frac{a}{a-1}}}$$

• Unlike global AdS, small BHs here are different than flat Schwartzschild ones as there is scalar hair.

• As functions of r_h, $E(r_h)$, $S(r_h)$ are monotonically decreasing functions, so that $E_{large}(T_i) > E_{small}(T_j)$ and $S_{large}(T_i) > S_{small}(T_j)$

• At a given energy $E \gg \Lambda_{YM}$, a large BH is preferentially created.

The entropy from the lattice at different N

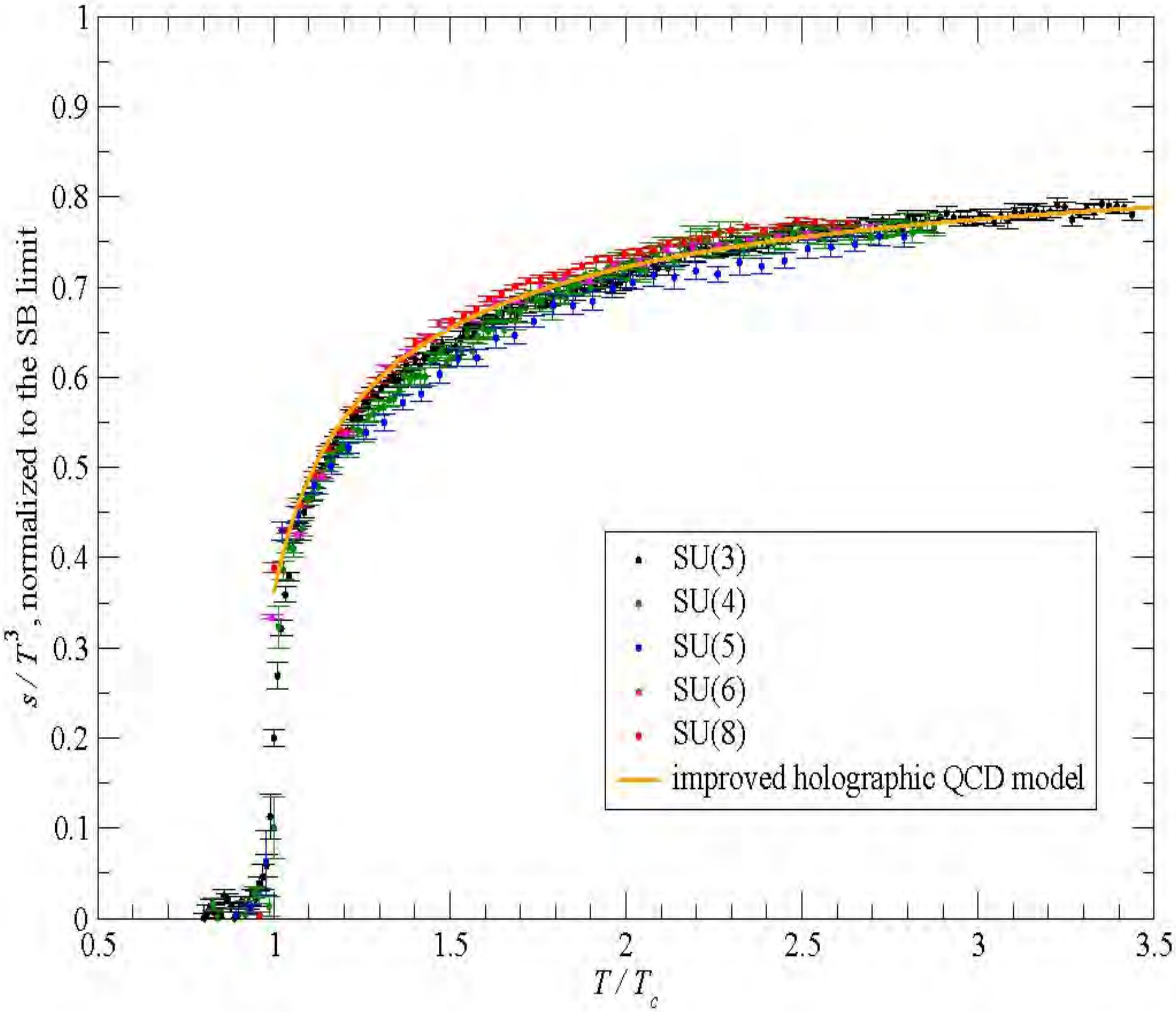

Figure 4: (Color online) Same as in fig. 1, but for the s/T^3 ratio, normalized to the SB limit.

Marco Panero arXiv: 0907.3719

The equation of state at different N

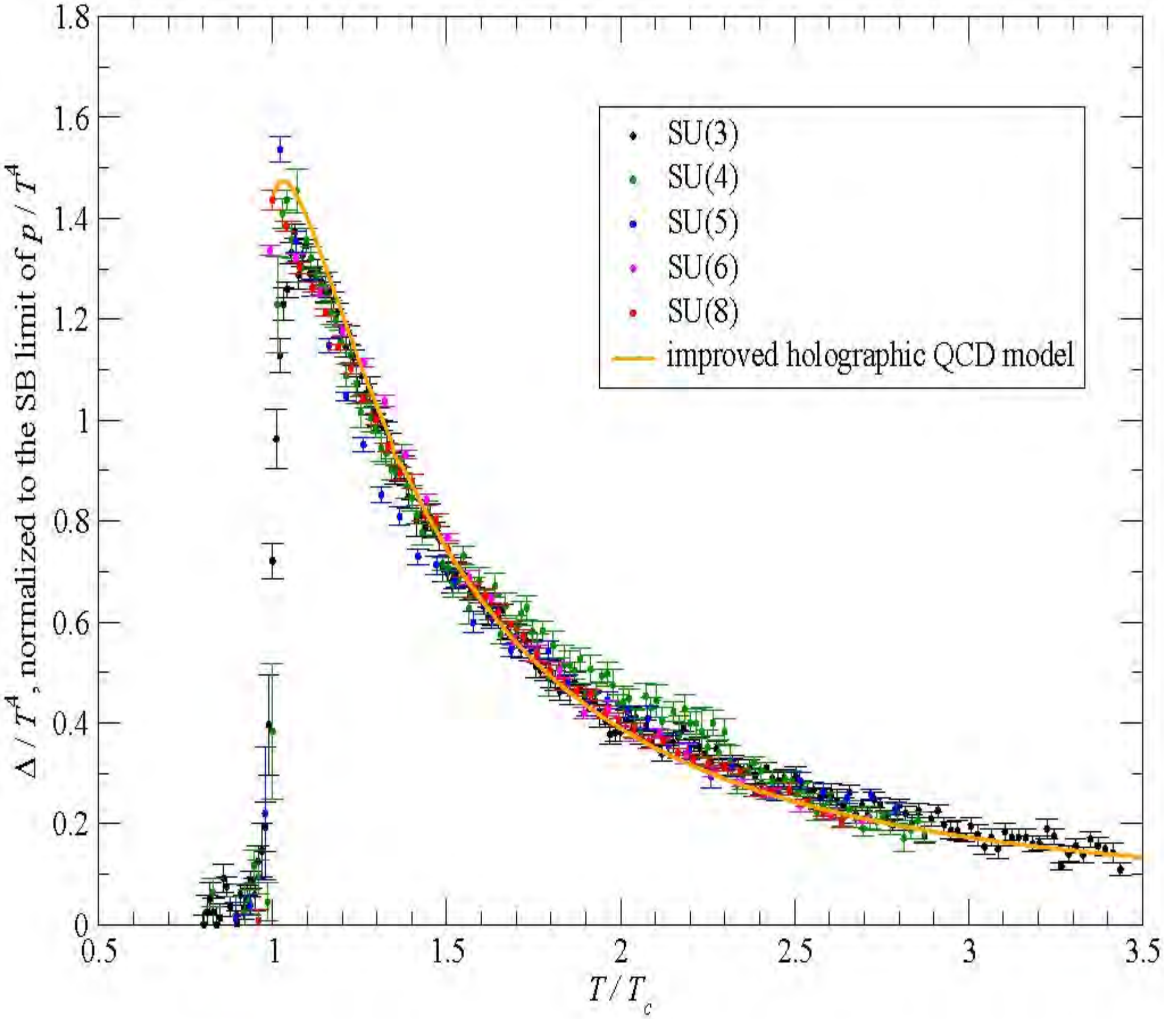

Figure 2: (Color online) Same as in fig. 1, but for the Δ/T^4 ratio, normalized to the SB limit of p/T^4.

Marco Panero arXiv: 0907.3719

The speed of sound

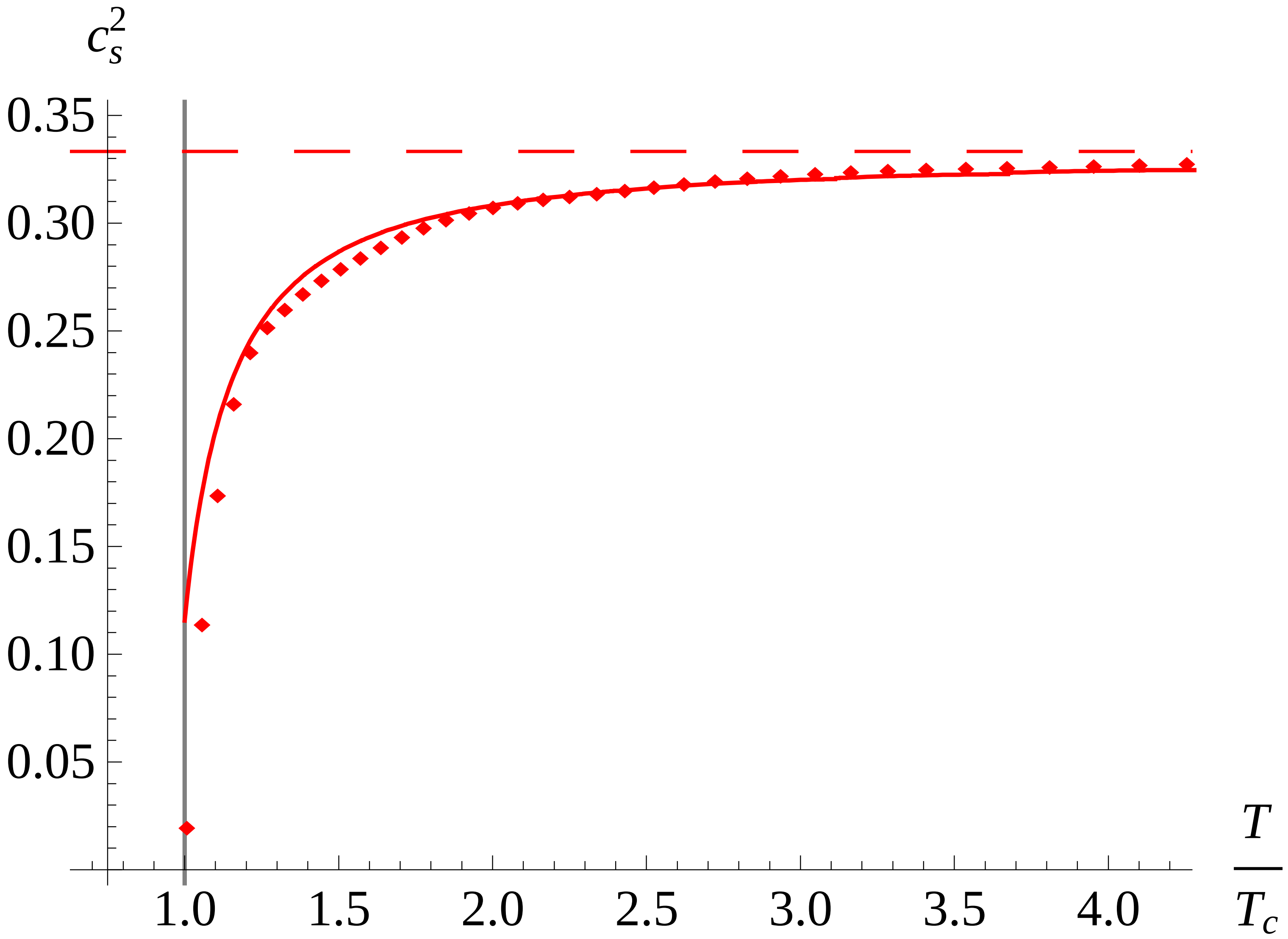

The phases of evolution in the bulk language

• 0.1 – 0.5 fm/c: deposition of about 20 TeV of energy (RHIC) in the midrapidity range. Density $\simeq$ 15 GeV/fm^3. Linear size $\simeq$ 10 fm

• 0.5 – 1 fm/c: Ultrafast thermalization and entropy production. In the gravitational picture formation of a trapped surface that leads to a horizon. The horizon is a ellipsoid with a cross section in the transverse plane and axis in the radial direction. The black hole generated is a "large" local BH.

• 1 – 6 fm/c: The BH is falling in the bulk space towards the center. Its shape in "comoving coordinates" is invariant, and therefore it entropy constant.

• Because of the warping, the size in transverse space expands in physical units while the size in the radial direction contracts (in physical units). This is an adiabatic expansion in 4d QCD terms.

- 6 − 10 fm/c: Almost isothermal expansion with $T = T_c$.

- In pure YM, during this period there are bubbles of the confining vacuum that materialize and grow, converting the QGP into hadrons. This is a distinct mechanism from Hawking evaporation as large black holes are thermodynamically stable.

- When massive quarks are present we have a steep crossover so the conversion is fuzzier, but qualitatively similar. This is harder to describe holographically.

- $>$ 10 fm/c: Hadrons fly off to detectors. During this and previous period, final state interactions are important for some observables especially HBT.

Thermalization and entropy production

• The thermalization proceeds in a strongly coupled medium.

• In the gravity picture it is signaled by the formation of a horizon.

• This is a highly non-linear process that even in Einstein gravity is difficult to calculate. Most of the progress is numerical and recent.

• Penrose has proposed a criterion for the formation of a horizon: the formation of a trapped surface. It is defined by a null conserved vector, $h^{\mu\nu}\nabla_\mu \ell^+_\nu = 0$. If it exists it evolves into a horizon.

• Its surface area $S_{trapped}$ gives a lower bound on the entropy S of the formed horizon

$$S_{trapped} \leq S$$

• In collisions of two shock waves, this surface can be calculated without having to solve the full non-linear problem.

It can be obtained from the solution of the problem

$$\Psi\Big|_C = 0 \quad , \quad \frac{1}{b(r)^2}\sum_{r,x_1,x_2}\nabla_i\Psi\nabla_i\Psi\Big|_C = 8 \quad , \quad ds^2 = b(r)^2(dr^2 + dx^\mu dx_\mu)$$

- Shocks without any transverse dependence.

$$\frac{1}{b^3(r_H)} = \sqrt{\frac{8}{s}} \quad , \quad S_{trapped} = \frac{A_\perp}{4G_5}\int_{r_H}^{\infty} b^3(r)dr$$

- Applying this to scaling, scale factors (quasiconformal, no mass gap) $b \sim \left(\frac{\ell}{r}\right)^a$, with $a \geq 1$, we obtain

$$S_{trapped} \sim s^{\frac{3a-1}{6a}}$$

The AdS case $a = 1$ agrees with:

Gubser+Pufu+Yarom

- For the YM related scale factors $b \sim e^{-(r\Lambda)^a}$, $a > 1$,

$$S_{trapped} \sim \sqrt{s}\,(\log[s])^{\frac{a+1}{a}}$$

• In QCD we expect that the strongly coupled description is valid up to a UV cutoff scale. Above this asymptotic freedom kicks in and suppresses entropy production. A way of taking this into account is to include the cutoff in the evaluation of the trapped surface area.

Gubser+Pufu+Yarom

• This procedure is ambiguous for shocks without transverse dependence.

• Shocks with power fall-off in transverse space:

For the YM related scale factors $b \sim e^{-(r\Lambda)^a}$, $a > 1$, and a UV cutoff we obtain

$$S_{trapped} \sim \log^2(s)$$

This is compatible with the Froissart bound.

• Recent numerical solution of the Einstein equations in AdS, found an approximate formula for the thermalization time

$$\tau_{th}\ \epsilon^{\frac{1}{4}} \simeq 0.65 \quad , \quad s_{final} = s_{initial} + 1.59\ s_{initial}^{1.55}$$

Heller+Janik+Witaszczyk

Outlook

• In have argued that RHIC and LHC heavy-ion collisions produce 5-dimensional black holes in the scalar-tensor gravity theory dual to QCD.

• Their production, some of their properties and decay are different from those expected from flat space mini-black holes.

• The arguments given here are semi-quantitative.

• Detailed solutions of finite size black holes, and their formation are lacking,(as they are difficult numerical problems)

• I have presented indications that theories that classicalize á la Dvali et al. may have a conventional QFT non-perturbative description, which is in agreement with classicalization in the right variables

• Eventual matching with experimental distributions of the multiplicities is necessary (we are on a good track)

• The final expectation: Use gravity to evolve the systems from 0.1 fm/c and onwards, up to hadronization for LHC.

.

Elliptic flow in pp ? (from CMS)

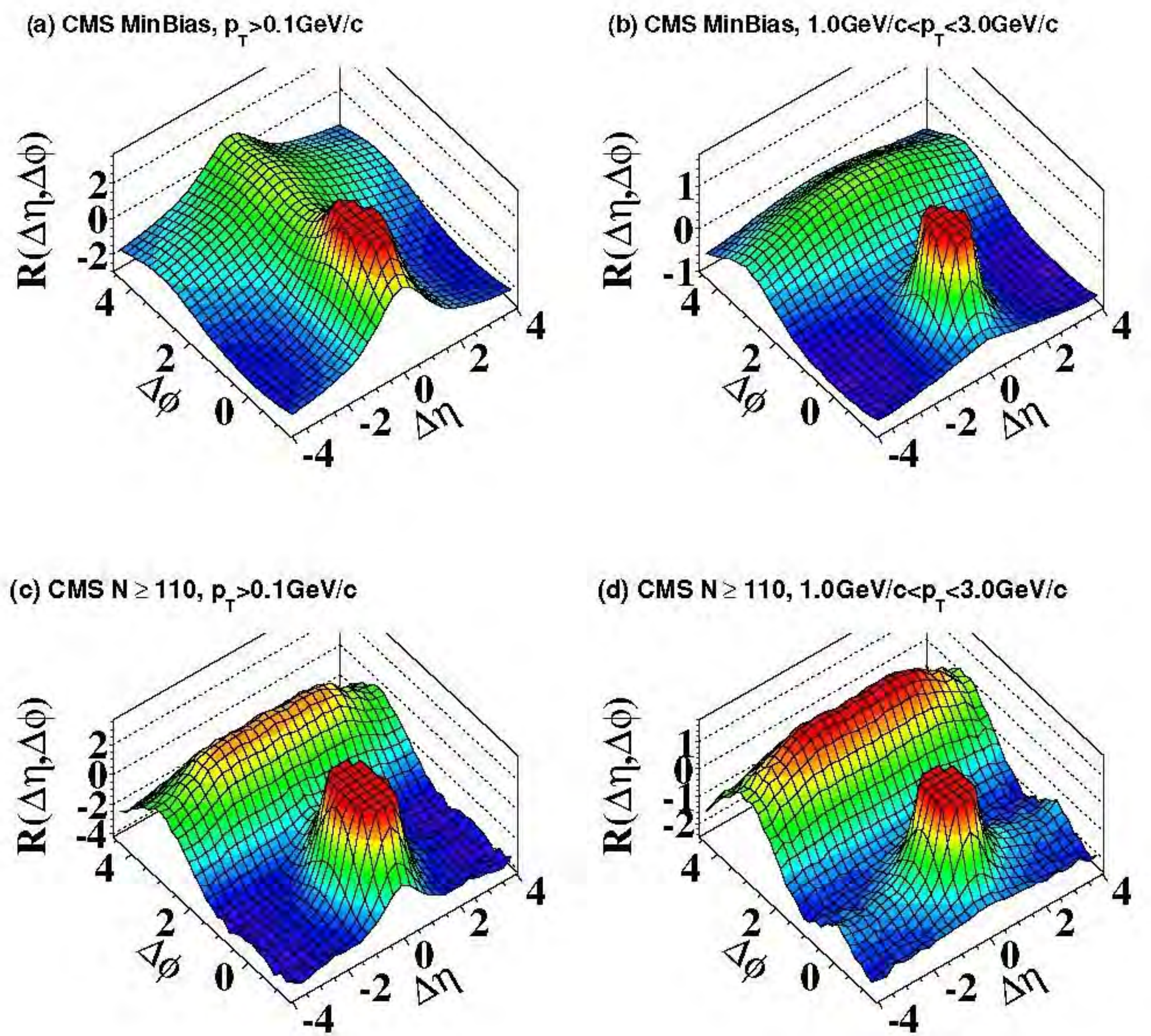

.

Thank you for your Patience

Trapped surfaces

A a surface S is called trapped if: Let ℓ_μ^+ be null, transverse to S and outward, and ℓ_μ^- be null, transverse to S and inward,

Define also the projective metric

$$h_{\mu\nu} = g_{\mu\nu} - \frac{\ell_\mu^+ \ell_\nu^- + \ell_\mu^- \ell_\nu^+}{g^{\rho\sigma} \ell_\rho^+ \ell_\sigma^-} \quad , \quad h^{\mu\nu} \ell_\nu^\pm = 0$$

The surface is trapped if

$$\theta = h^{\mu\nu} \nabla_\mu \ell_\nu^+ = 0$$

RETURN

The pressure from the lattice at different N

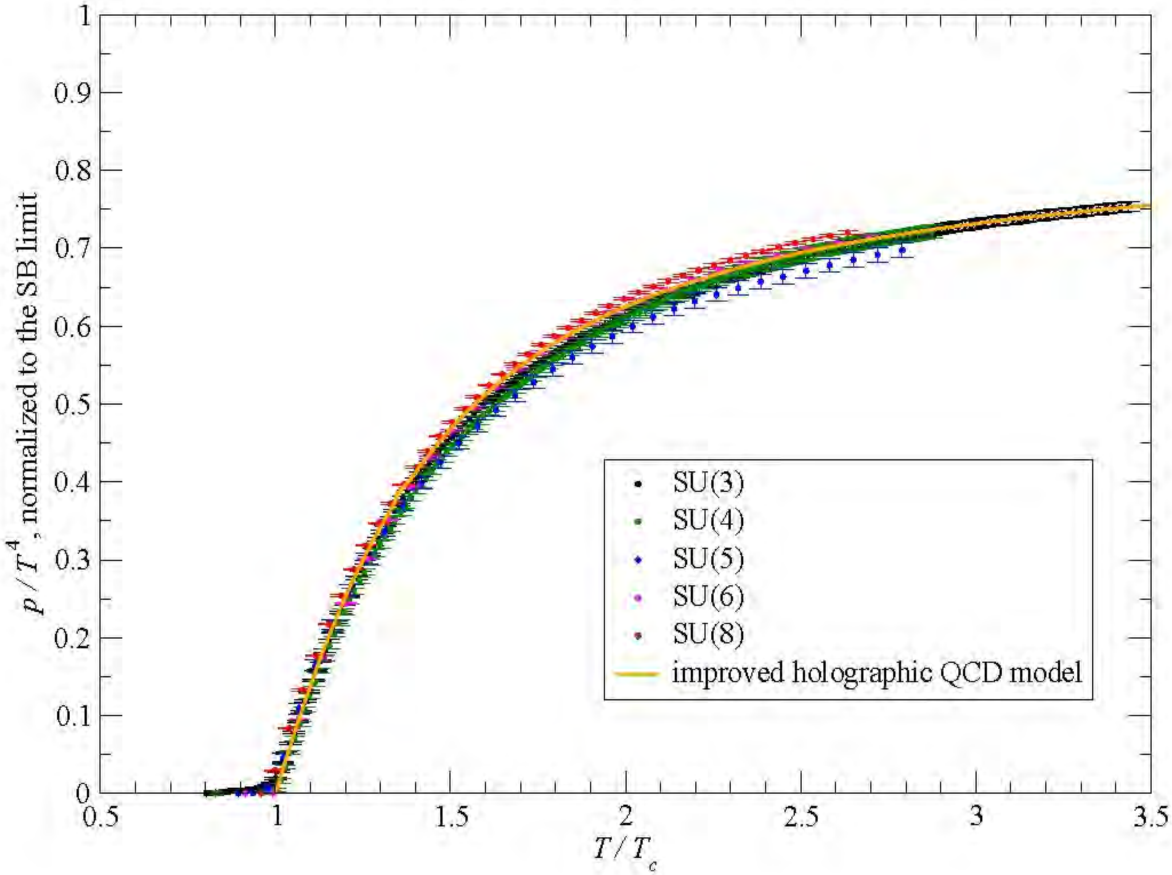

Figure 1: (Color online) The dimensionless ratio p/T^4, normalized to the lattice SB limit $\pi^2(N^2-1)R_I(N_t)/45$, *versus* T/T_c, as obtained from simulations of $SU(N)$ lattice gauge theories on $N_t = 5$ lattices. Errorbars denote statistical uncertainties only. The results corresponding to different gauge groups are denoted by different colors, according to the legend. The yellow solid line denotes the prediction from the improved holographic QCD model from ref. [75] (with a trivial, parameter-free rescaling to our normalization).

Marco Panero arXiv: 0907.3719

The Bjorken Relation

- Consider that after the collision of the nuclear pancakes a lot of particles are produced at $t = \tau$. These are confined in a slice of longitudinal width dz and transverse area A.

- The longitudinal velocities have a spread $dv_L = \frac{dz}{\tau}$.

- Near the middle region $v_L \to 0$

$$\frac{dy}{dv_L} = \frac{d}{dv_L}\left[\frac{1}{2}\log\frac{1+v_L}{1-v_L}\right] = \frac{1}{1-v_L^2} \simeq 1$$

- We may now write

$$dN = dv_L\ \frac{dN}{dv_L} \simeq \frac{dz}{\tau}\ \frac{dN}{dy} \quad \to \quad \frac{dN}{dz} \simeq \frac{1}{\tau}\ \frac{dN}{dy}$$

- If $\langle E_T\rangle \simeq \langle m_T\rangle$ is the average energy per particle then the energy density in this area at $t = \tau$ is given by the Bjorken formula:

$$\langle\epsilon(\tau)\rangle \simeq \frac{dN\langle m_T\rangle}{dz\ \ A} = \frac{1}{\tau}\frac{dN}{dy}\frac{\langle m_T\rangle}{A} = \frac{1}{\tau\ A}\frac{dE_T^{\text{total}}}{dy}$$

- It is valid if (1) τ can be defined meaningfully (2) The crossing time $\ll \tau$.

RETURN

The mid-rapidity range

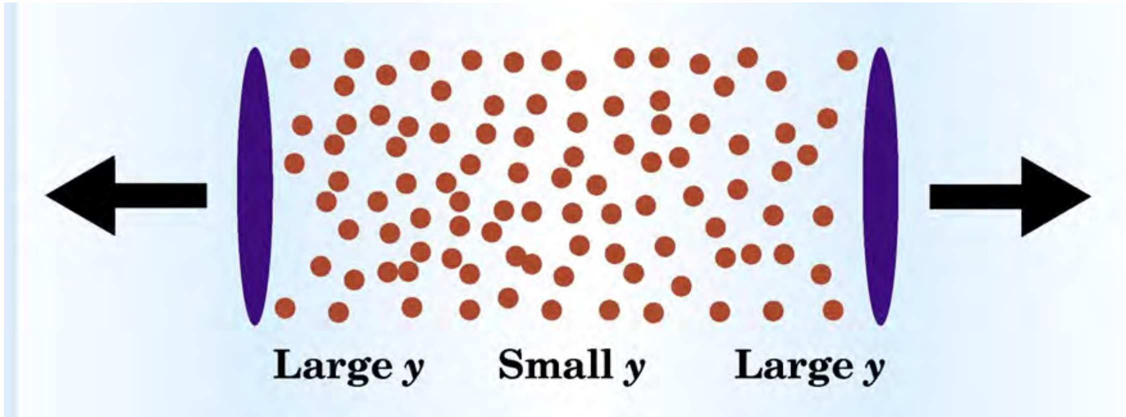

- The crossing time for Au nuclei (with radius 8 fm) is $\sim$ 0.1fm/c $\simeq$ 3×10^{-25} seconds.

- The particles with small v_L are produced after 1 fm/c $\simeq$ 3×10^{-24} seconds. Those with higher v_L are produced later due to time dilation.

- Use the rapidity variable $y = \frac{1}{2} \log \left[\frac{1+\frac{v_L}{c}}{1-\frac{v_L}{c}} \right]$. Δy is Lorentz invariant.

- The "new matter" (free of fragments) is produced near $y \simeq 0$. This is what we are looking for.

- This can be tested by looking at how much "baryon" number is at mid-rapidity

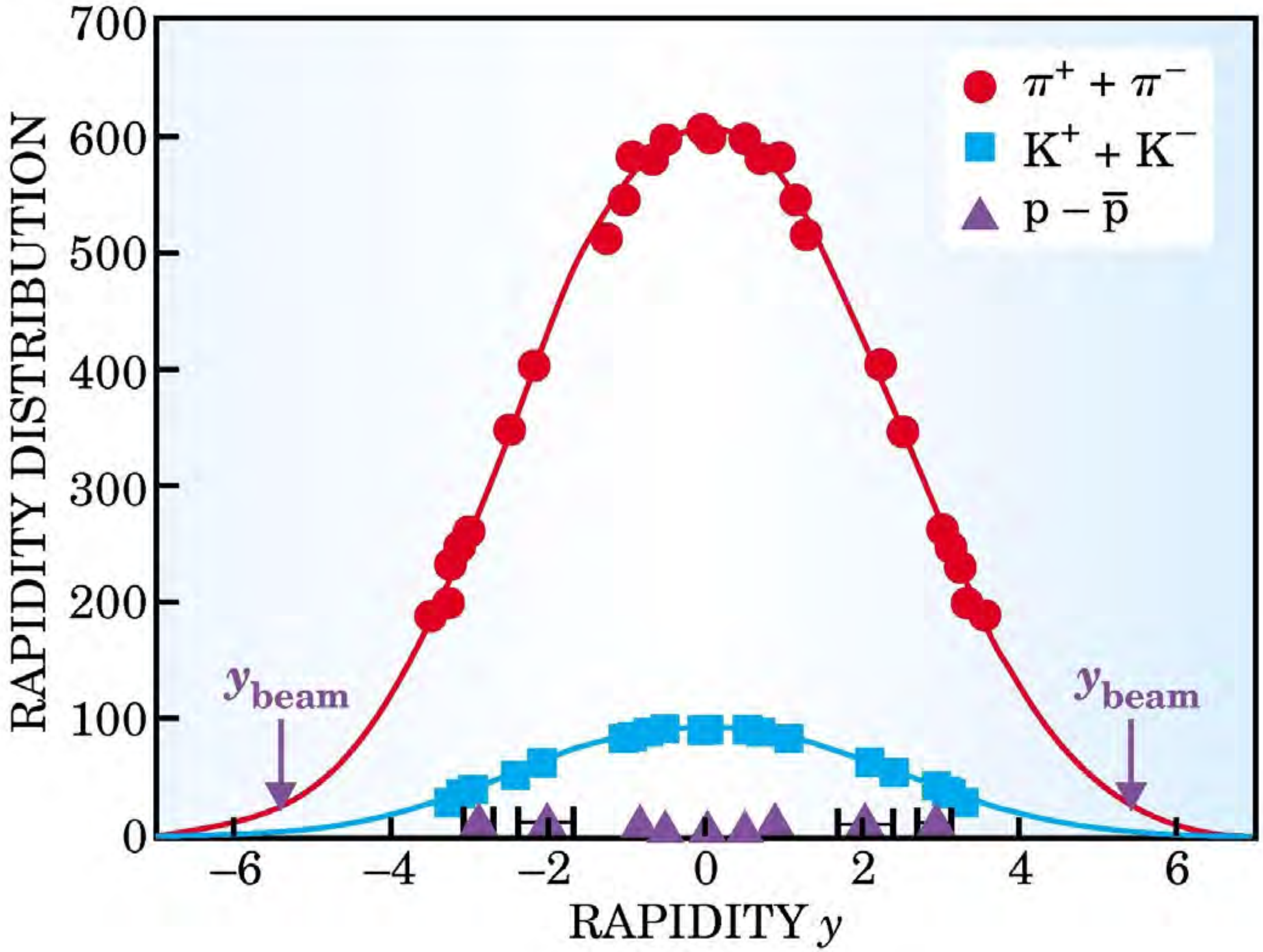

• Distribution of zero baryon number and net baryon number particles as a function of rapidity (from BRAHMS)

• Each beam nucleon looses 73 ± 6 GeV on the average that goes into creating new particles. Therefore there is 26 TeV worth of energy available for particle production.

Ellipticity

Ollitrault, 1992

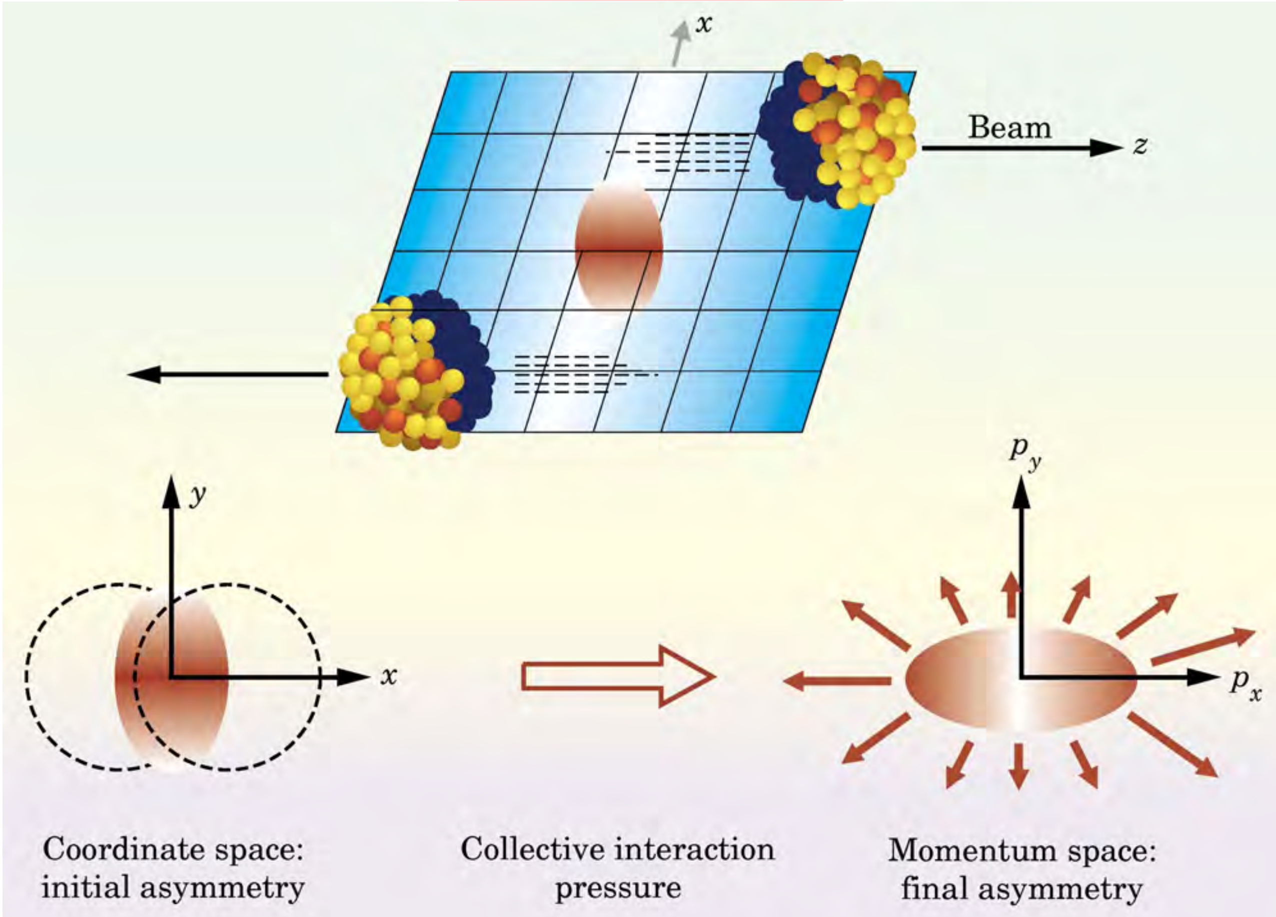

- In an off-center collision, an initial elliptic pattern is produced.

- If the subsequent interactions are weak particles are free streaming and this elliptic pattern is wiped-out

- If the interactions are strong, this pattern persists and is visible in the detectors.

Elliptic flow

$$\frac{1}{p_T}\frac{dN}{dp_T\,d\phi} = \frac{1}{p_T}\frac{dN}{dp_T}\,(1 + 2\,v_2(p_T)\cos(2\,\phi) + ...)$$

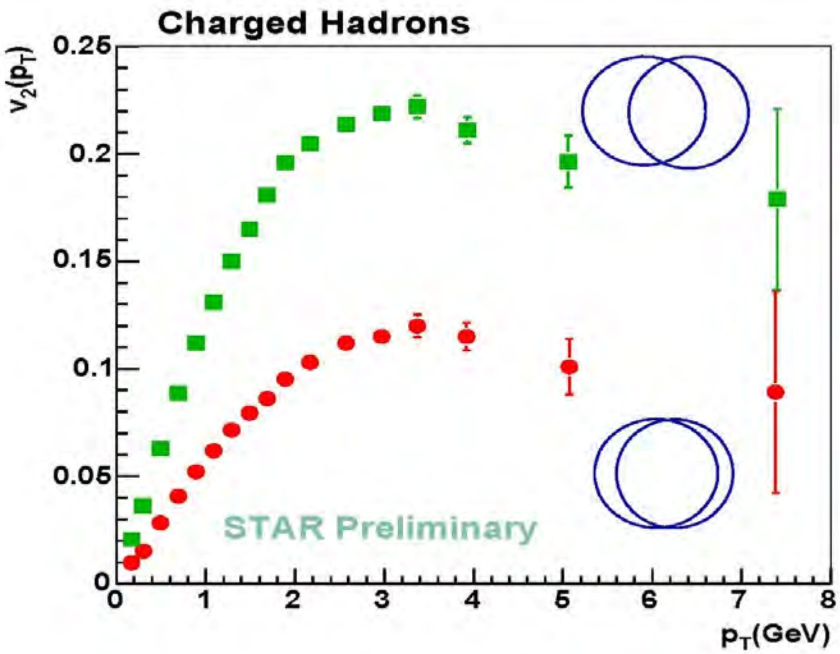

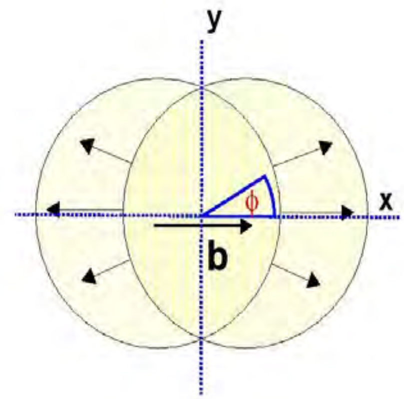

X:Y = $(1 + \underbrace{2v_2}_{\sim 0.4} : 1 - \underbrace{2v_2}_{\sim 0.4})$

Elliptic flow is large X:Y $\sim 2.0 : 1$

- Such Elliptic flow has been observed recently in strongly coupled cold gases.

Elliptic flow in ultracold gases

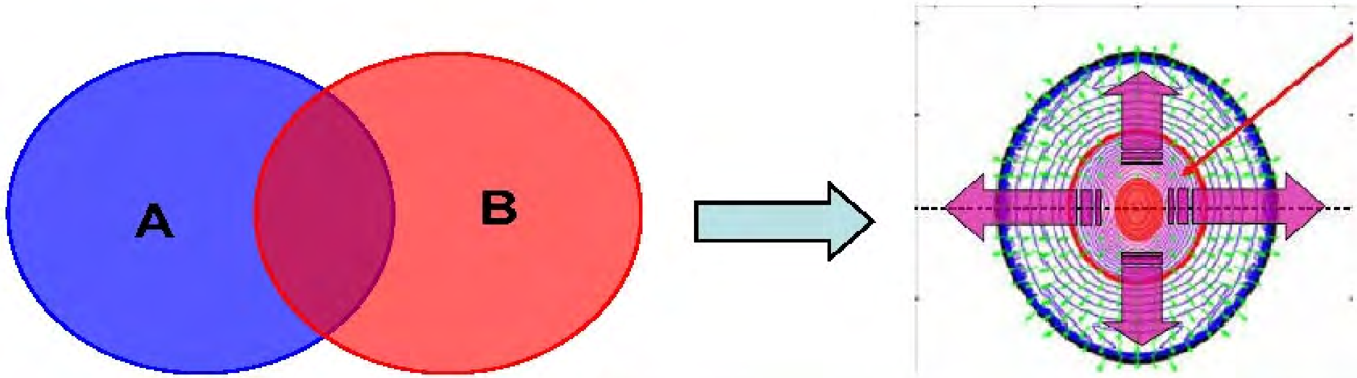

Na_{23}

Bose condensate

Ketterle group, MIT

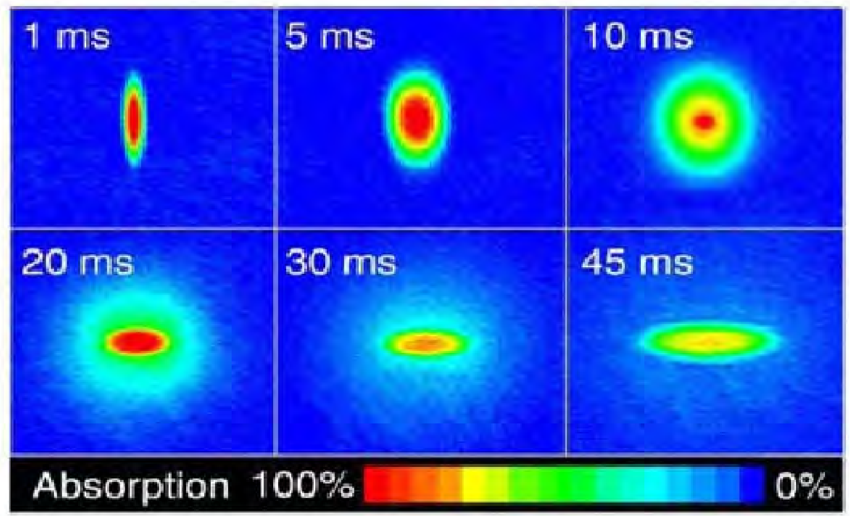

The UV region

Choose a monotonic potential with UV asymptotics (no minima).

$$\lim_{\lambda\to 0} V(\lambda) = \frac{12}{\ell^2}\left(1+\sum_{n=1}^{\infty} c_n\lambda^n\right) = \frac{12}{\ell^2}\left(1+c_1\lambda+c_2\lambda^2+\cdots\right)$$

- The Poincaré invariant ansatz is

$$ds^2 = b(r)^2(dr^2+dx^\mu dx_\mu) \quad , \quad \lambda\to\lambda(r)$$

- The small λ asymptotics generate the UV expansion around AdS_5:

$$\frac{1}{\lambda} = -b_0\log(r\Lambda)+\cdots \quad , \quad b\equiv e^A = \frac{\ell}{r}\left[1+\frac{2}{9\log(r\Lambda)}+\cdots\right]$$

- There is a 1-1 correspondence between the holographic "YM" β-function, $\beta(\lambda)$ and W defined as $\left(\frac{3}{4}\right)^3 V(\lambda) = W^2 - \left(\frac{3}{4}\right)^2\left(\frac{\partial W}{\partial\log\lambda}\right)^2$:

$$\frac{d\lambda}{d\log E} = \beta(\lambda) = -\frac{9}{4}\lambda^2\,\frac{d\log W(\lambda)}{d\lambda} = -b_0\lambda^2+b_1\lambda^3+\cdots$$

with $E = e^A$

The fit to glueball lattice data

J^{PC}	Ref I (MeV)	Our model (MeV)	Mismatch	$N_c \to \infty$	Misn
0^{++}	**1475 (4%)**	**1475**	0	**1475**	0
2^{++}	2150 (5%)	2055	4%	2153 (10%)	5
0^{-+}	**2250 (4%)**	**2243**	0		
0^{++*}	**2755 (4%)**	**2753**	0	2814 (12%)	2
2^{++*}	2880 (5%)	2991	4%		
0^{-+*}	3370 (4%)	3288	2%		
0^{++**}	3370 (4%)	3561	5%		
0^{++***}	3990 (5%)	4253	6%		

Comparison between the glueball spectra in Ref. I and in our model. The states we use as input in our fit are marked in red. The parenthesis in the lattice data indicate the percent accuracy.

The glueball wavefunctions

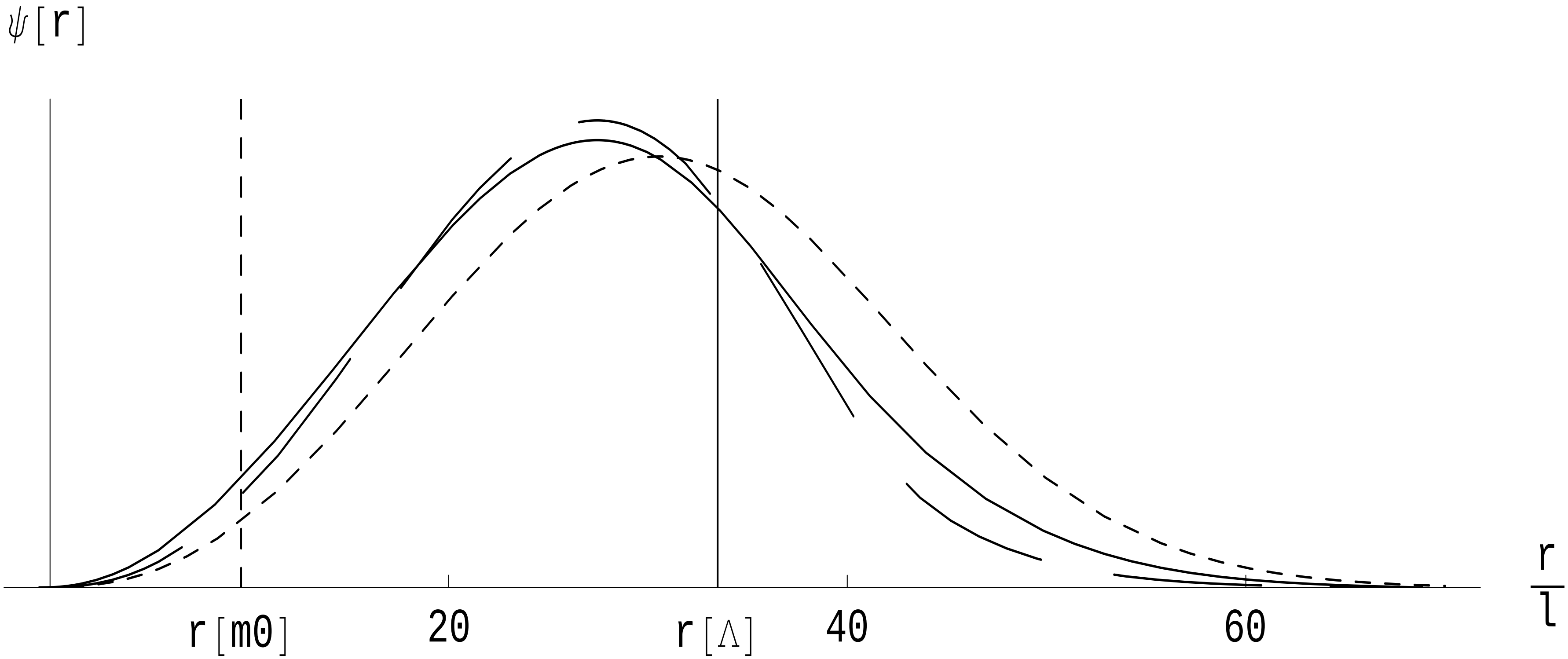

Normalized wave-function profiles for the ground states of the 0^{++} (solid line) ,0^{-+} (dashed line), and 2^{++} (dotted line) towers, as a function of the radial conformal coordinate. The vertical lines represent the position corresponding to $E = m_{0^{++}}$ and $E = \Lambda_p$.

The lattice glueball data

J^{++}	Ref. I $(m/\sqrt{\sigma})$	Ref. I (MeV)	Ref. II (mr_0)	Ref. II (MeV)	$N_c \to \infty(m$
0	3.347(68)	1475(30)(65)	4.16(11)(4)	1710(50)(80)	3.37(15)
0^*	6.26(16)	2755(70)(120)	6.50(44)(7)	2670(180)(130)	6.43(50)
0^{**}	7.65(23)	3370(100)(150)	NA	NA	NA
0^{***}	9.06(49)	3990(210)(180)	NA	NA	NA
2	4.916(91)	2150(30)(100)	5.83(5)(6)	2390(30)(120)	4.93(30)
2^*	6.48(22)	2880(100)(130)	NA	NA	NA
R_{20}	1.46(5)	1.46(5)	1.40(5)	1.40(5)	1.46(11)
R_{00}	1.87(8)	1.87(8)	1.56(15)	1.56(15)	1.90(17)

Available lattice data for the scalar and the tensor glueballs. Ref. I =H. B. Meyer, [arXiv:hep-lat/0508002]. and Ref. II = C. J. Morningstar and M. J. Peardon, [arXiv:hep-lat/9901004] + Y. Chen *et al.*, [arXiv:hep-lat/0510074]. The first error corresponds to the statistical error from the the continuum extrapolation. The second error in Ref.I is due to the uncertainty in the string tension $\sqrt{\sigma}$. (Note that this does not affect the mass ratios). The second error in the Ref. II is the estimated uncertainty from the anisotropy. In the last column we present the available large N_c estimates according to B. Lucini and M. Teper, [arXiv:hep-lat/0103027]. The parenthesis in this column shows the total possible error followed by the estimations in the same reference.

Free energy versus horizon position

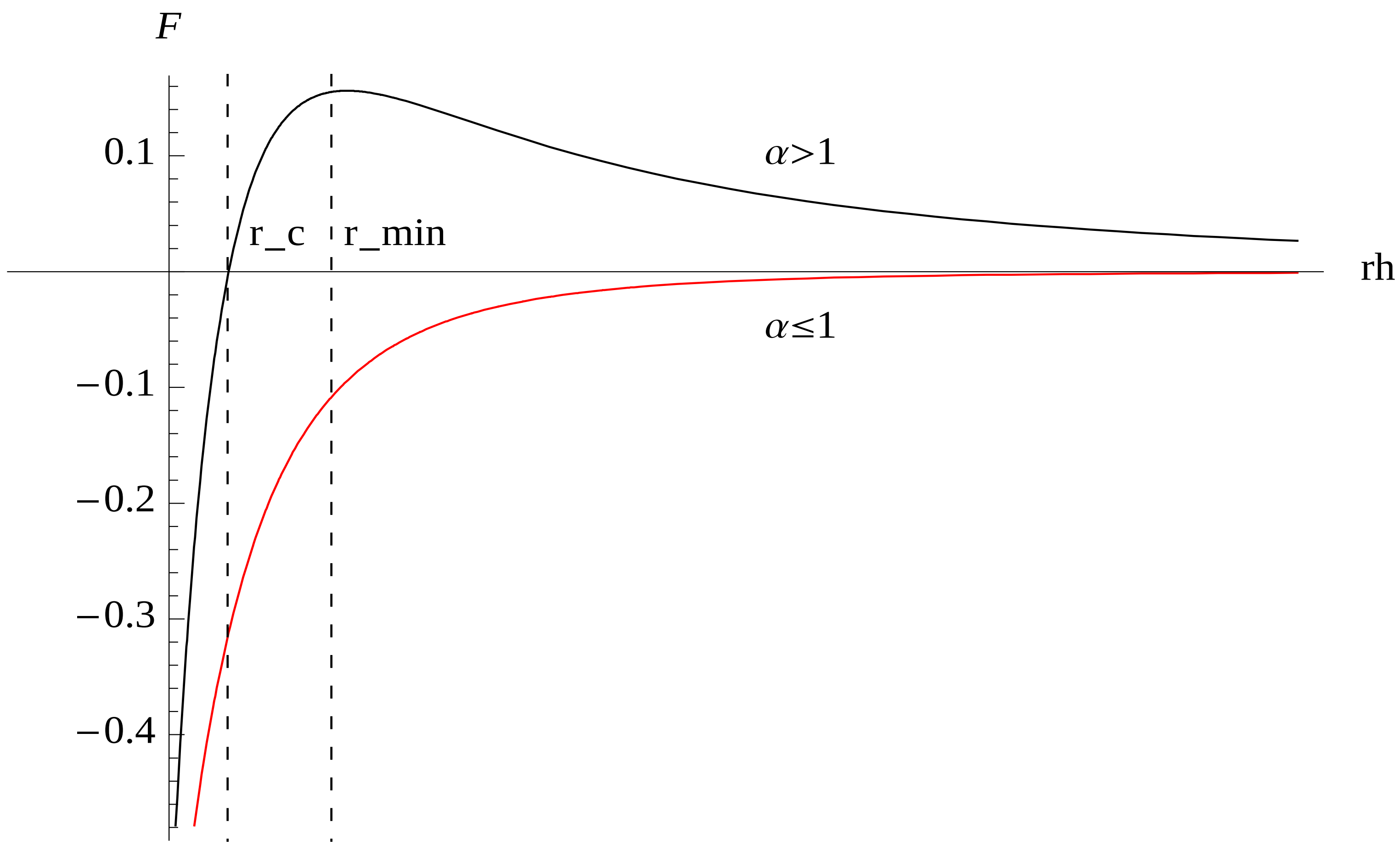

We plot the relation $\mathcal{F}(r_h)$ for various potentials parameterized by a. $a = 1$ is the critical value below which there is no first order phase transition .

The transition in the free energy

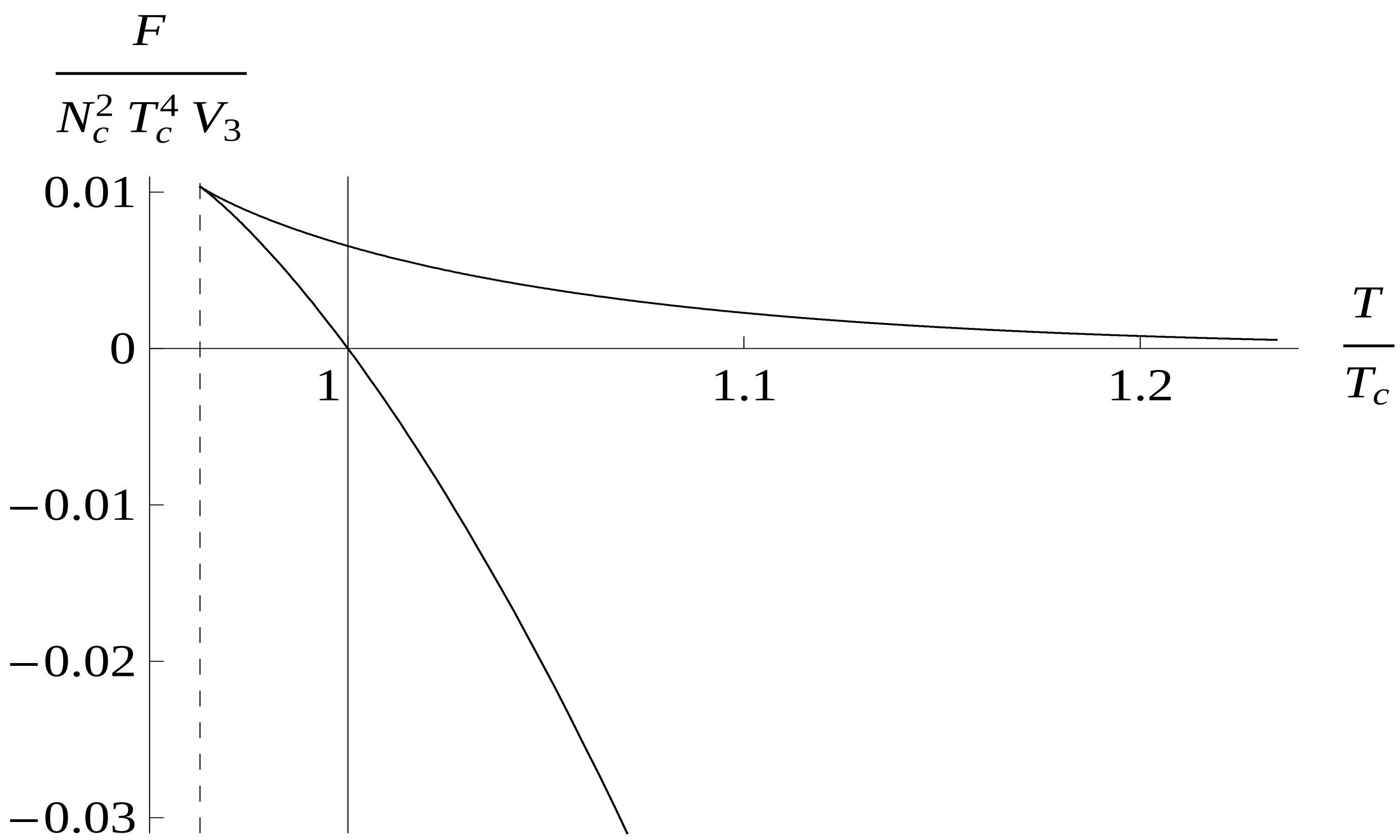

- G. Boyd, J. Engels, F. Karsch, E. Laermann, C. Legeland, M. Lutgemeier and B. Petersson, *"Thermodynamics of SU(3) Lattice Gauge Theory,"* Nucl. Phys. B **469**, 419 (1996) [arXiv:hep-lat/9602007].

- B. Lucini, M. Teper and U. Wenger, *"Properties of the deconfining phase transition in SU(N) gauge theories,"* JHEP **0502**, 033 (2005) [arXiv:hep-lat/0502003];
"SU(N) gauge theories in four dimensions: Exploring the approach to $N = \infty$," JHEP **0106**, 050 (2001) [arXiv:hep-lat/0103027].

- Y. Chen *et al.*, *"Glueball spectrum and matrix elements on anisotropic lattices,"* Phys. Rev. D **73** (2006) 014516 [arXiv:hep-lat/0510074].

- L. Del Debbio, L. Giusti and C. Pica, *"Topological susceptibility in the SU(3) gauge theory,"* Phys. Rev. Lett. **94**, 032003 (2005) [arXiv:hep-th/0407052].

RETURN

Comparison with lattice data

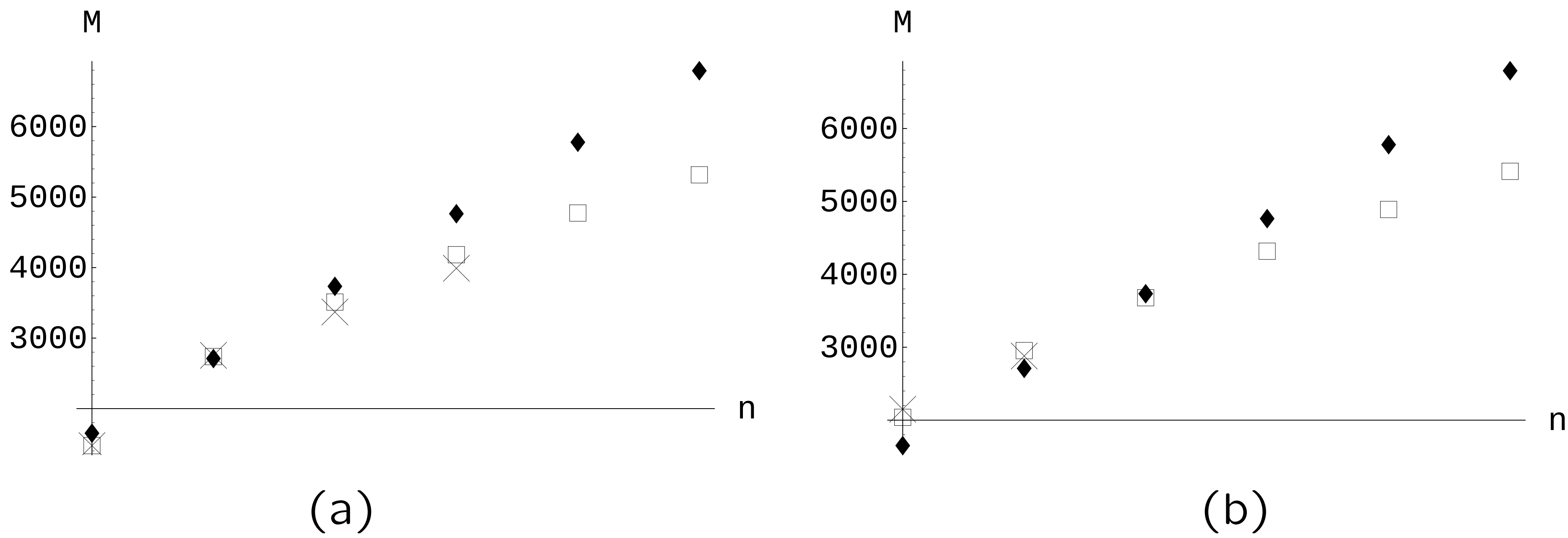

Linearity of the glueball spectrum

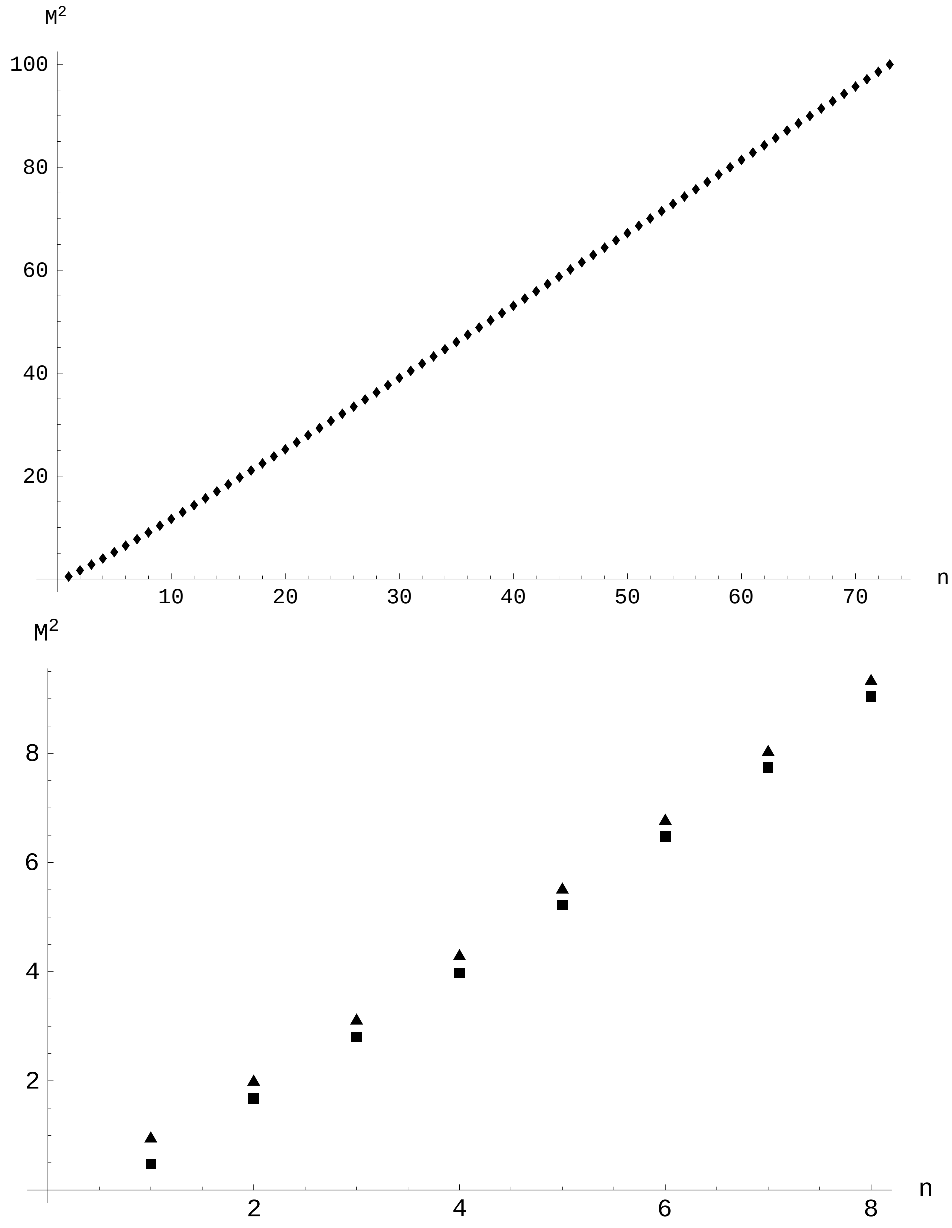

(a) (b)

(a) Linear pattern in the spectrum for the first 40 0^{++} glueball states. M^2 is shown units of $0.015\ell^{-2}$.

(b) The first 8 0^{++} (squares) and the 2^{++} (triangles) glueballs. These spectra are obtained in the background I with $b_0 = 4.2, \lambda_0 = 0.05$.

Comparison with lattice data (Meyer)

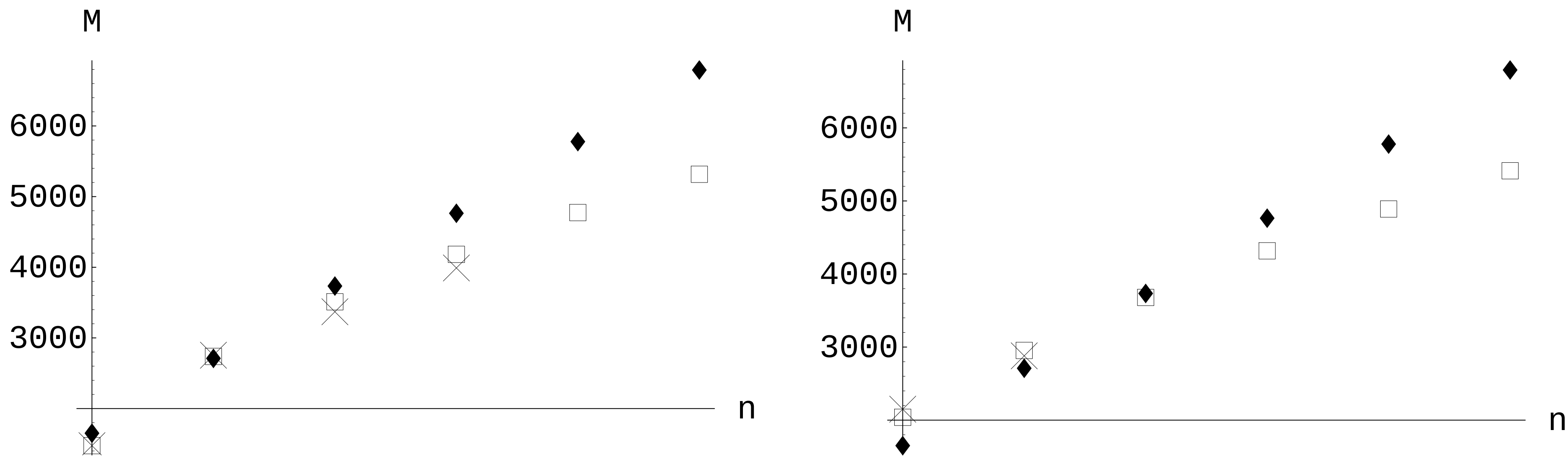

(a) (b)

Comparison of glueball spectra from our model with $b_0 = 4.2, \lambda_0 = 0.05$ (boxes), with the lattice QCD data from Ref. I (crosses) and the AdS/QCD computation (diamonds), for (a) 0^{++} glueballs; (b) 2^{++} glueballs. The masses are in MeV, and the scale is normalized to match the lowest 0^{++} state from Ref. I.

Parameters

• We have 3 initial conditions in the system of graviton-dilaton equations:

♠ One is fixed by picking the branch that corresponds asymptotically to $\lambda \sim \frac{1}{\log(r\Lambda)}$

♠ The other fixes $\Lambda \to \Lambda_{QCD}$.

♠ The third is a gauge artifact as it corresponds to a choice of the origin of the radial coordinate.

• We parameterize the potential as

$$V(\lambda) = \frac{12}{\ell^2}\left\{1 + V_0\lambda + V_1\lambda^{4/3}\left[\log\left(1 + V_2\lambda^{4/3} + V_3\lambda^2\right)\right]^{1/2}\right\},$$

• We fix the one and two loop β-function coefficients:

$$V_0 = \frac{8}{9}b_0 \quad , \quad V_2 = b_0^4\left(\frac{23 + 36 b_1/b_0^2}{81 V_1^2}\right)^2 , \quad \frac{b_1}{b_0^2} = \frac{51}{121}.$$

and remain with two leftover arbitrary (phenomenological) coefficients.

• We also have the Planck scale M_p
Asking for correct $T \to \infty$ thermodynamics (free gas) fixes

$$(M_p \ell)^3 = \frac{1}{45\pi^2} \quad , \quad M_{\text{physical}} = M_p N_c^{\frac{2}{3}} = \left(\frac{8}{45\pi^2 \ell^3}\right)^{\frac{1}{3}} \simeq 4.6 \text{ GeV}$$

• The fundamental string scale. It can be fixed by comparing with lattice string tension

$$\sigma = \frac{b^2(r_*)\lambda^{4/3}(r_*)}{2\pi\ell_s^2},$$

$\ell/\ell_s \sim \mathcal{O}(1)$.

• ℓ is not really a parameter as it can be rescaled into a redefinition of λ.

♠ In the CP-odd sector (axion) there are two more parameters:

$$Z(\lambda) = Z_0(1 + c_a \lambda^4)$$

Fit and comparison

	IhQCD	lattice $N_c = 3$	lattice $N_c \to \infty$	Parameter
$[p/(N_c^2 T^4)]_{T=2T_c}$	**1.2**	**1.2**	-	$V1 = 14$
$L_h/(N_c^2 T_c^4)$	**0.31**	0.28 (Karsch)	**0.31** (Teper+Lucini)	$V3 = 170$
$[p/(N_c^2 T^4)]_{T\to+\infty}$	$\pi^2/45$	$\pi^2/45$	$\pi^2/45$	$M_p \ell = [45\pi^2]^{-1/3}$
$m_{0^{++}}/\sqrt{\sigma}$	**3.37**	3.56 (Chen)	**3.37** (Teper+Lucini)	$\ell_s/\ell = 0.92$
$m_{0^{-+}}/m_{0^{++}}$	**1.49**	**1.49** (Chen)	-	$c_a = 0.26$
χ	$(191 MeV)^4$	$(191 MeV)^4$ (DelDebbio)	-	$Z_0 = 133$
$T_c/m_{0^{++}}$	0.167	-	0.177(7)	
$m_{0^{*++}}/m_{0^{++}}$	1.61	1.56(11)	1.90(17)	
$m_{2^{++}}/m_{0^{++}}$	1.36	1.40(4)	1.46(11)	
$m_{0^{*-+}}/m_{0^{++}}$	2.10	2.12(10)	-	

Spatial string tension

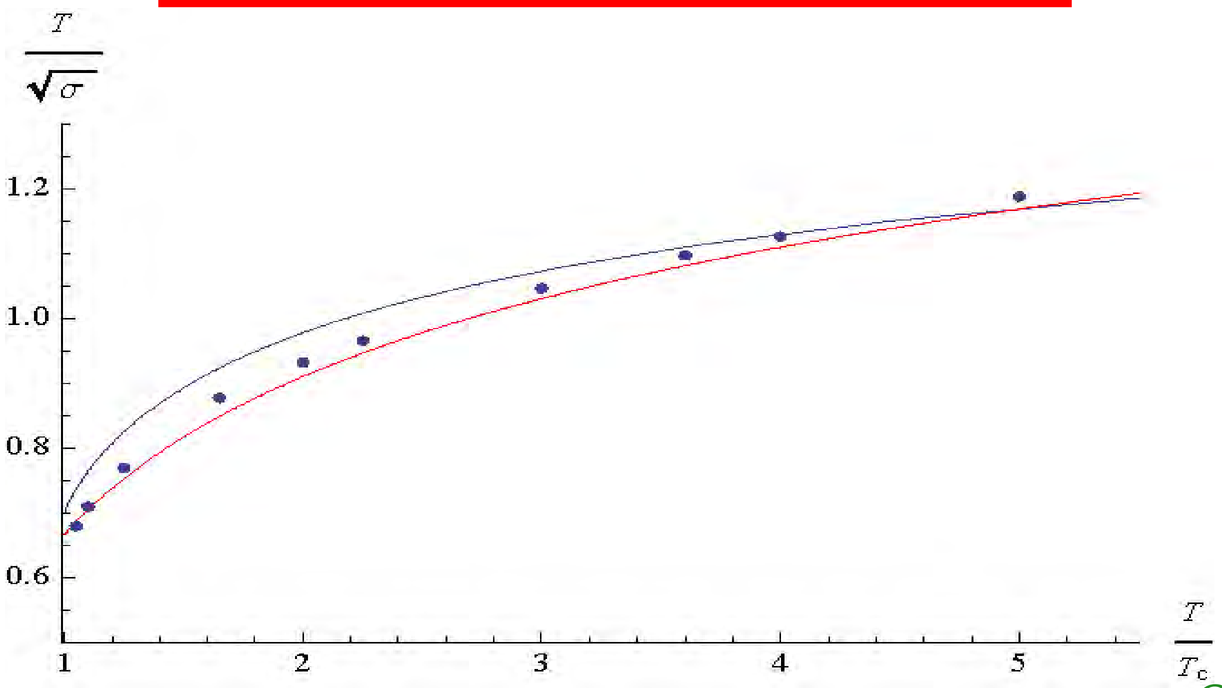

G. Boyd et al. 1996

• The blue line is the spatial string tension as calculated in Improved hQCD, with no additional fits.

Nitti (unpublished) 2009

• The red line is a semi-phenomenological fit using

$$\frac{T}{\sqrt{\sigma_s}} = 0.51 \left[\log\frac{\pi T}{T_c} + \frac{51}{121}\log\left(2\log\frac{\pi T}{T_c}\right)\right]^{\frac{2}{3}}$$

Alanen+Kajantie+Suur-Uski, 2009

Detailed plan of the presentation

- Title page 1 minutes
- Collaborators 2 minutes
- Introduction 4 minutes
- Preview 7 minutes
- RHIC head-on collision 8 minutes
- Phases of a collision 10 minutes
- Is there thermal equilibrium? 11 minutes
- Hydrodynamic elliptic flow 13 minutes
- Improved Holographic QCD 14 minutes
- The IR asymptotics 16 minutes
- The general phase structure 17 minutes
- Temperature versus horizon position 19 minutes
- The thermodynamics of small vs large BHs 21 minutes

- The entropy 22 minutes
- The equation of state 23 minutes
- The speed of sound 23 minutes
- Thermalization and entropy production 27 minutes
- Outlook 28 minutes

- Trapped Surfaces 29 minutes
- The YM pressure 30 minutes
- The Bjorken Relation 31 minutes
- The mid-rapidity range 34 minutes
- Ellipticity 35 minutes
- Elliptic flow 37 minutes
- Elliptic flow in ultracold gases 39 minutes
- The UV region 42 minutes
- The fit to Meyer Lattice data 43 minutes
- The glueball wavefunctions 44 minutes
- The lattice glueball data 45 minutes
- The free energy versus horizon position 46 minutes
- The transition in the free energy 47 minutes
- Comparison with lattice data 49 minutes
- Linearity of the glueball spectrum 50 minutes
- Comparison with lattice data (Meyer) 51 minutes

- Parameters 54 minutes
- Fit and comparison 57 minutes
- Spatial string tension 58 minutes